A Flexible All-Atom Model of Dimethyl Sulfoxide for Molecular Dynamics Simulations

Matthew L. Strader and Scott E. Feller*

Department of Chemistry, Wabash College, Crawfordsville, Indiana 47933

Received: October 1, 2001

An all-atom, flexible dimethyl sulfoxide model has been created for molecular dynamics simulations. The new model was tested against experiment for an array of thermodynamic, structural, and dynamic properties. Interactions with water were compared with previous simulations and experimental studies, and the unusual changes exhibited by dimethyl sulfoxide/water mixtures, such as the enhanced structure of the solution, were reproduced by the new model. Particular attention was given to the design of the electrostatic component of the force field and to providing compatibility with the CHARMM parameter sets for biomolecules.

Introduction

Theoretical methods for the investigation of biological molecules have become commonplace in biochemistry and biophysics.[1] These approaches provide detailed atomic models of biological systems, from which structure−function relationships can be elucidated. Methods based on empirical force fields, such as molecular dynamics (MD) simulations, allow for calculations on relatively large systems, e.g., complete biomolecules or assemblies of biomolecules in their aqueous environment. For example, molecular dynamics computer simulation techniques have proven to be particularly valuable for studying the structure and dynamics of lipid bilayer membranes.[2] They have found use in providing information that is complementary to laboratory experiments and useful in the interpretation of diffraction[3] and NMR[4] data by providing a detailed picture of the membrane with extremely high spatial and temporal resolution.

The interaction of dimethyl sulfoxide (DMSO) with lipid bilayer membranes and other biological macromolecules is a subject of interest due both to fundamental biophysical questions of solvent−solute interactions, and due to its considerable practical importance. For example, aqueous DMSO has been found to induce cell fusion[5] and to increase membrane permeability,[6] and to serve as an important cryoprotectant[7] and radioprotectant.[8] It is not surprising that aqueous mixtures of DMSO have significant effects on biomolecules, given that mixtures of DMSO and water exhibit highly nonideal physical properties upon mixing, such as decreased density, longer rotational reorientation relaxation times, lower diffusion coefficients, and negative changes in molar enthalpy and volume. For example, an interesting and useful cryoprotective property is the freezing point of −62 °C for a 1:3 DMSO:H_2O mixture. Hypotheses proposed to explain the nonideality of mixing typically involve the hydrogen bonding structure of water and the DMSO oxygen,[9−13] but direct experimental evidence of such theories is difficult to obtain.

MD simulations are well suited to analyze DMSO, its interactions with water, and its effects on macromolecular assemblies. A number of groups have already utilized this technique for the study of neat DMSO,[14−16] its aqueous mixtures,[14,17,18] and its interaction with a phospholipid bilayer.[19,20] Simulations published to date have utilized a rigid, united-atom model where each methyl group is represented by a single atomic center and all bond lengths and angles are fixed at their equilibrium values. Another feature common to most of these models is the use of the same charge distribution, namely that obtained by Rao and Singh from a Hartree−Fock 6-31G* ab initio quantum mechanical calculation.[21]

Recent advances in computer hardware now allow a flexible, all-atom DMSO molecule to be simulated with reasonable computational expense. Thus, we have undertaken the development of intramolecular energy parameters for this molecule. Because a goal of this work was to develop a DMSO model useful for lipid bilayer simulations, and a previous simulation of this system identified substantial changes in the membrane electrostatic potential upon replacing water with DMSO,[20] we also worked to determine a set of atomic charges that reproduced a variety of electrostatic force field dependent properties. Finally, our model was designed to be consistent with the Chemistry at HARvard Molecular Mechanics (CHARMM)[22,23] all-atom parameter set.[24] To this end, parameters for the DMSO methyl group were taken directly from the CHARMM27 lipid parameters and the DMSO-water potential was taken into account explicitly by studying the DMSO-TIP3P water model interaction energy. By following the parameter development philosophy upon which the CHARMM biomolecular force field is based,[23] the DMSO model should be suitable for simulations of proteins, nucleic acids, and lipids.

In the following we describe in detail the parametrization of our new DMSO model, hereafter referred to as FS (Feller−Strader). The next section gives the computational details of the calculations on isolated DMSO, neat DMSO liquid, and aqueous DMSO solutions. This is followed by a detailed comparison of simulation results with those of previous models and with experiment, for quantities such as density, enthalpy of vaporization, translational diffusion constants, reorientational correlation times, viscosity, dielectric constant, surface tension, radial distribution functions, and ΔH and ΔV of mixing for aqueous DMSO solutions. The final section summarizes these results and describes potential applications of this work. A subsequent publication will describe our results on a DMSO/water/lipid system.

* Corresponding author. Telephone 765-361-6175. Fax 765-361-6340. E-mailfellers@wabash.edu.

10.1021/jp013658n CCC: $22.00
Published on Web 01/12/2002

Methods

Quantum Mechanical (QM) Calculations. Ab initio QM calculations were performed with the programs Gaussian 98[25] and PCSpartanPro.[26] Gaussian 98 was used to calculate the torsional energy surface for methyl rotation at the MP2/6-31G-(d) level of theory by fixing the O−S−C−H dihedral in increments of 12° and carrying out a geometry optimization of the remaining degrees of freedom. PCSpartanPro was used to calculate the vibrational frequencies and atomic charges at the HF/6-31+G* level of theory. The higher level calculations were used on the torsional energy surface to better account for electronic correlation effects that could contribute to the interactions between atoms separated by more than one chemical bond, while the normal-mode analysis was done at the Hartree−Fock level and scaled by a factor of 0.89 to correct for electron correlation.[27] Atomic charges were calculated using the electrostatic fitting procedure.[28] The potential energy of interaction between DMSO and water was calculated from the difference in QM energies of a gas-phase DMSO-water complex and the isolated molecules. The complex was studied by carrying out a geometry optimization in PCSpartanPro at the HF/6-31+G* level with the intramolecular geometry of each molecule kept fixed. This level of theory was used to maintain uniformity with solute-water interaction energies for other components of the CHARMM parameter set. The QM interaction energy was scaled by 1.16, also in accord with the parameter development methodology employed for CHARMM27, to account for polarization effects.[29]

Empirical Energy Calculations. The program CHARMM was employed for all force field calculations. It utilizes the following empirical energy function:[24]

$$U_{\text{tot}} = \sum_{\text{bonds}} k_b(b - b_0)^2 + \sum_{\text{angle}} k_\theta(\theta - \theta_0)^2 + \sum_{\text{dihedrals}} k_\phi[\cos(n\phi - \delta) + 1] + \sum_{\text{nonbonded}} \left\{ \frac{q_i q_j}{4\pi\epsilon_0 r_{ij}} + \epsilon\left[\left(\frac{\sigma}{r_{ij}}\right)^{12} - \left(\frac{\sigma}{r_{ij}}\right)^{6}\right]\right\}$$

where b is the bond length, θ is the bond angle, ϕ is the torsion angle, and r_{ij} is the distance between atomic centers; k_b, k_θ, k_ϕ, are the force constants for bond distortion, angle distortion, and torsional rotation, respectively; q is the atomic charge; and ϵ and σ are the Lennard-Jones parameters.

Gas-phase simulations were performed on a single molecule without periodic boundary conditions. For the gas-phase calculations, no truncation of the nonbonded interactions was performed. The heat of vaporization was calculated by adding the difference in internal energies in the gas and liquid phases (ΔU) to the difference in PV (assumed to equal RT) to obtain a difference in enthalpy (ΔH). To calculate the empirical interaction energy for the water−DMSO complex, the ab initio optimized coordinates were read into CHARMM, and the interaction energy calculated.

Condensed phase simulations were carried out in a cubic cell, with periodic boundary conditions, for four systems: pure DMSO, a 1:3 DMSO/TIP3P mole ratio mixture, a 4:1 DMSO/TIP3P mole ratio mixture, and pure TIP3P. A simulation of the DMSO liquid/vapor interface was carried out to obtain the surface tension[30] employing a tetragonal simulation cell. Table 1 gives a description of the size of each system. The Lennard-Jones (LJ) potential was switched smoothly to zero over the region from 10 to 12 Å. Electrostatic interactions were included via the smooth particle mesh Ewald summation.[31] All bonds involving hydrogen were fixed at their equilibrium distances using the SHAKE algorithm.[32] A time step of 2 fs was employed with a leapfrog Verlet integration scheme. A neighbor list, used for calculating the LJ potential and the real space portion of the Ewald sum, was kept to 14 Å and updated every 20 fs. A variant of the extended system formalism, the Langevin Piston algorithm, was used to control pressure at 1 atm.[33] The temperature was maintained at 30 °C by means of the Hoover thermostat.[34,35] Coordinates sets were saved every 1 ps for subsequent analysis (see following paragraph). Simulations were carried out using 1−4 processors on a Beowulf-type parallel computer. Total simulation lengths were 1.3 ns for the neat DMSO, 1.1 ns for the two mixtures and the neat water, and 10 ns for gas-phase simulations.

TABLE 1: Description of Simulation Systems Used

simulations	approximate cell dimension (Å)	no. of DMSO molecules	no. of TIP3P molecules
neat DMSO	34.1	326	0
1:3 DMSO:WATER	32.2	161	483
4:1 DMSO:WATER	32.0	256	64
neat TIP3P	25.6	0	560

Condensed Phase Simulation Analysis Calculations. A number of experimentally measurable properties were calculated from the condensed phase simulations, in each case these quantities were calculated from the last nanosecond of simulation trajectory. For single molecule properties, the reported results represent an averaging over molecules and over the simulation trajectory.

Rotational reorientation correlation times, τ, were calculated by integrating the autocorrelation function of the second Legendre polynomial, $C(t) = \langle P_2(\mu(0))\cdot P_2(\mu(t))\rangle$, from $t = 0$ to the point at which the correlation function reaches zero.[35] Radial distribution functions, $g_{ij}(r)$, were calculated from normalized histograms of the distances between the various atom pairs. Weighted sums of radial distributions functions for heavy atoms were calculated with scaling factors from Luzar et al.[15] to compare with experimental neutron scattering data. The mean squared displacement correlation function, $C(t) = (R(t) - R(t + \tau))^2$, was used to calculate the translational diffusion constant (D). Linear least-squares fitting was used to obtain a line of the form $y = 6D^*t + b$, in the diffusive regime from 5 to 100 ps, using the standard deviations among the molecules as weights.[30] Viscosity (η) was calculated using the Einstein-Helfand relation,[36]

$$\frac{2\eta kT}{V}t = \langle[\textstyle\int_0^t P_{\alpha\beta}(t')\,\mathrm{d}t']^2\rangle \qquad (1)$$

where $P_{\alpha\beta}$ is the off-diagonal component of the pressure tensor, k is the Boltzman constant, T is the absolute temperature, V is the simulation cell volume, and t is the time. The right-hand side of eq 1 was calculated for each off-diagonal element and then averaged. The standard deviation among the three elements was determined, and the average in the interval $t = 1-100$ ps was fitted to the equation using the standard deviations as weights.[37] The dielectric constant (ϵ) was calculated from

$$\epsilon = 1 + \frac{4\pi}{3Vk_{\text{B}}T}\left(\left\langle\left|\sum_{i=1}^{N}\mu_i\right|^2\right\rangle - \left\langle\left|\sum_{i=1}^{N}\mu_i\right|\right\rangle^2\right) \qquad (2)$$

where μ_i is the dipole moment.[38] Surface tension was calculated from the difference in the normal and tangential components of the pressure tensor.[30] The changes in enthalpy (ΔH) and

TABLE 2: Final Force Field Parameters for the FS Model of DMSO

Nonbonded Parameters

atom	charge	ϵ_{min} (kcal/mol)	$R_{min}/2$ (Å)
H	0.090	−0.024	1.34
C	−0.148	−0.078	2.04
S	0.312	−0.350	2.00
O	−0.556	−0.120	1.70

Bond Parameters

bond	k_b (kcal/mol·Å^2)	b_0 (Å)
H−C	322	1.11
C−S	240	1.80
S−O	540	1.53

Angle Parameters

angle	k_θ [kcal/(mol·rad^2)]	θ_0 (deg)
H−C−H	35.5	108.4
H−C−S	46.1	111.3
C−S−O	79.0	106.75
C−S−C	34.0	95.0

Dihedral Parameters

dihedral angle	k_ϕ (kcal/mol)	n	δ (deg)
H−C−S−O	0.2	3	0
H−C−S−C	0.2	3	0

volume (ΔV) upon mixing were determined by comparing the volume and enthalpy of the mixed system to the volumes and enthalpies of the corresponding simulated neat liquids. The values are reported on a per mole of solution basis.

Results and Discussion

Parametrization of Intramolecular Energy Terms. Because the FS model is to our knowledge the first flexible model of DMSO, the design process necessarily required an evaluation of force constants for bond stretching, angle bending, and dihedral rotation. Additionally, the use of an all-atom model required that parameters for all terms involving hydrogen atoms be developed. Data from several sources were incorporated into the model; however, to maintain uniformity with the lipid parameter set, values from version 27 of the CHARMM lipid and protein parameter sets[24,39] were used wherever feasible. The final set of parameters is given in Table 2.

The equilibrium bond lengths, bond angles, and associated force constants were obtained primarily from the CHARMM parameter set. All methyl group bond and angle parameters were taken from the CHARMM alkane methyl potential. The C−S−C bond angle, the C−S bond length and their respective force constants were taken from the CHARMM values employed in the methionine amino acid residue. The methionine sulfur was selected because it, like DMSO, is sp^3 hybridized and bonded to two saturated alkane groups. Although this equilibrium angle (95°) appears slightly smaller than the 97.4° value employed in the OPLS,[40] P2[15] and NPS[14] models, it should be noted that the flexibility of the present model allows the possibility that the angle observed in the simulation is not necessarily the parameter value. The average C−S−C angle observed in the neat DMSO simulation is 98.5° (Figure 1). Studies summarized by Vaisman and Berkowitz[17] on various methods used to determine the C−S−C angle give values ranging from 96.6 to 100.4°. Thus, the simulation value falls well within the range of experimental values. Methyl sulfate provides the closest model compound in the CHARMM parameter set for the S−O bond parameters. Although, the CHARMM parameter for the

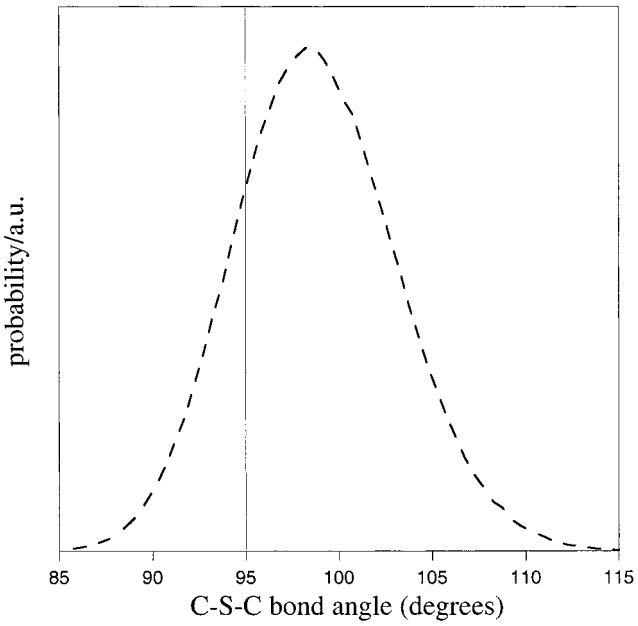

Figure 1. Distribution of C−S−C bond angles in the simulation of neat DMSO liquid (dashed line). The solid line gives the value of θ_0 in the potential energy function.

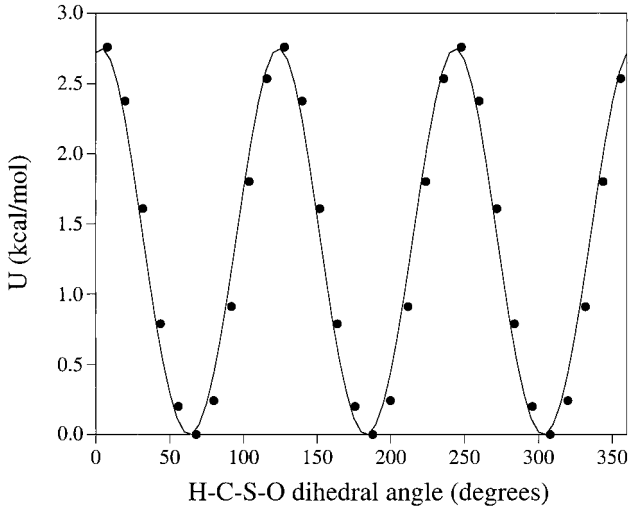

Figure 2. Quantum mechanical (symbols) and empirical (solid line) potential energy surfaces for the H−C−S−O dihedral angle.

force constant can accurately model DMSO (as judged from the comparison of ab initio and empirical vibrational frequencies), the bond length of S−O in methyl sulfate is nearly 0.1 Å smaller than the solid-state bond length obtained from X-ray diffraction.[41] Thus the X-ray diffraction value of 1.53 Å was adopted for the equilibrium S−O bond length. The same X-ray diffraction study also provided the C−S−O equilibrium angle value of 106.75° for which no similar CHARMM parameter existed. Finally, the C−S−O force constant was chosen by matching the empirical vibrational frequencies calculated by CHARMM to the ab initio vibrational frequencies at 311.63 and 360.64 cm^{-1} (the modes dominated by the C−S−O angle bending motion). The methyl rotation barrier was parametrized using a single cosine function with 3-fold periodicity by fitting the empirical potential energy surface to the ab initio results (Figure 2), yielding a rotational barrier of approximately 2.75 kcal/mol. The empirical vibrational frequency calculation utilizing the final parameter values was in good agreement with the ab initio data, yielding an RMS difference of 4%.

TABLE 3: Comparison of Experimental and Simulation Results for Physical Properties of Pure DMSO

property	exp	present work	united atom models[14,16]
density (g/cm^3)[a]	1.091	1.071	1.078−1.099
ΔH_{vap} (kJ/mol)[a]	52.8	55.8	51.32−52.87
D (10^{-9} m^2/s)[a]	0.95	0.64	0.89−1.15
τ_{SO} (ps)[b]	5.2	4.3	3.0−3.9
τ_{CH} (ps)[b]	3.4	2.6	N/A
dielectric constant[c]	46.4	40.4	30
viscosity (cP)[c]	1.99	2.11	1.26
surface tension (dyn/cm)[c]	43.0	34.6	N/A

[a] Vishyakov et al.[14] [b] Kowalewski and Kovacs.[12] [c] Rao and Singh.[21]

Parametrization of Intermolecular Energy Terms. The intermolecular terms are the result of compromises that provide the best agreement with experimental data for the wide range of physical properties given in Table 3, with particular attention given to the electrostatic component of the force field to ensure accurate interactions with water and with the polar groups typical of biomolecules. A large number of atomic charge sets were tested including those employed in previously published DMSO models. The final charges were based on the results of the ab initio calculations that produced a gas-phase dipole of 4.22 D, which is in reasonable agreement with the experimental dipole of 4.06 D. A modification of the methyl hydrogen and carbon charges was made in order to make all methyl hydrogens equivalent and to give the methyl group identical charges to the existing CHARMM alkane potential. This adjustment gave an empirical dipole moment of 5.11 D, approximately 20% larger than the experimental value. This overestimation is consistent with other models of polar substances, is typical of other model compounds using the CHARMM force field, and partially accounts for polarization effects.[24] The Lennard-Jones well depths (ϵ_{min}) and radii (R_{min}) came directly from the CHARMM parameter set for hydrogen, carbon and oxygen atoms. Final adjustment of the FS model was made by testing ~20 DMSO models (varying sulfur well depths and radii, and atomic charges) each of length 400 ps, against experimental data. The interaction energy of DMSO with water obtained with the final parameter set suggest that DMSO-water interactions can also be reproduced with the final force field.

Simulation Results for Neat DMSO Liquid. The present model reproduces well the experimentally measured properties of DMSO (Table 3). The density is within 2% of the experimental value and is slightly low, a discrepancy that is related to the truncation of attractive Lennard-Jones forces outside the cutoff region and will decrease with a greater cutoff distance. It is encouraging that properties that depend strongly on Coulombic interactions, such as the heat of vaporization, dielectric constant and surface tension, are well reproduced by the simulation. The compromise between the various pieces of target data, however, is clearly evident. For example, the heat of vaporization is a few kcal/mol too large, suggesting that the liquid is somewhat too attractive. The calculated surface tension, however, is smaller than experiment suggesting insufficient molecular attractions. Particularly satisfying is the good agreement between simulation and experiment for the dielectric constant, a property that is extremely sensitive to details of the potential and which presumably is intimately involved in determining the solvation of charged and polar biomolecules.

The rotational relaxation of DMSO, as measured by the relaxation of the C−H and S−O bond vectors, agrees well with the experimental values and is significantly more accurate than other reported models.[14] The ratio of S−O relaxation time to C−H relaxation time is within 9% of the experimental ratio,[12] suggesting that the barrier to methyl rotation barrier is reasonably well parametrized. The somewhat low translational diffusion constant and slightly high viscosity (2.11 vs 1.99 cP) both suggest that the molecules are diffusing too slowly; however, the agreement with experiment is at a level typical of polar liquids.

TABLE 4: Comparison of Experimental and Simulation Results for Physical Properties of DMSO/Water Mixtures at Concentrations of $X_{DMSO} = 0.25$ and $X_{DMSO} = 0.80$'

	$X = 0.25$			$X = 0.80$	
property	exp	present work	united atom models[14]	exp	present work
density (g/cm^3)	1.077[a]	1.057	1.031−1.064	N/A	1.073
ΔH_{mix} (kJ/mol)	−2.96[a]	−4.76	−0.74- −2.65	N/A	−1.32
ΔV_{mix} (cm^3/mol)	−0.833[a]	−0.417	−0.185- −0.501	N/A	−0.165
D_{DMSO} (10^{-9} m^2/s)	0.61[a]	0.52	0.51−1.23	N/A	0.55
D_{water} (10^{-9} m^2/s)	1.01[a]	1.02	0.71−2.55	N/A	0.54
τ_{SO} (ps)	12.5[a]	10.2	2.8−5.4	6.4[b]	7.1
τ_{CH} (ps)	5.3[b]	3.6	N/A	3.9[b]	3.1
τ_{OH} (ps)	8.3[b]	5.8	2.8−4.1	6.3[b]	10.9

[a] Vishyakov[14] et al. [b] Kowalewski and Kovacs.[12]

Table 4 provides data on aqueous DMSO mixtures at concentrations of $X_{DMSO} = 0.25$ and $X_{DMSO} = 0.80$, and shows good agreement with experiment. The density of the mixtures is slightly low, as expected given the simulated density of neat DMSO. The translational and rotational mobility of both components are in excellent agreement with the experimental values. In this respect, the FS model is a great improvement over other DMSO models tested in 1:3 DMSO/water mixtures.[14] The translation and rotation of the TIP3P water in solution with the FS DMSO is also more accurate than previous DMSO/water combinations. The combination of a higher simulated ΔV_{mix} value and a lower ΔH_{mix} value than observed experimentally is the only shortcoming of the present DMSO-water interaction; however, this too results from a compromise among target experimental data. If both values were too low, the results would indicate that the water/DMSO interaction was too strong. Similarly, if both values were too high, the data would tend to indicate that the water/DMSO interaction was too weak. The present results suggest a more subtle adjustment of the water-DMSO potential is required to reproduce the true interactions. It has been shown that other DMSO models simulated with TIP3P water at this ratio also underestimate the ΔV_{mix}[14] so this shortcoming of the FS model is not unusual. As the concentration of DMSO increases, the density, diffusion coefficient and DMSO reorientation relaxation times move away from the 0.25 mole fraction values and toward the pure DMSO values. Again, the data from the simulation are in good agreement with experiment although less experimental data exist at this concentration. The greatest discrepancy is the rather long rotational reorientation time for water in the mixture, but it is difficult to assign this inaccuracy to shortcomings in the water or DMSO model.

The structure of DMSO, both as a neat liquid and in aqueous solution, is of great importance in understanding its many interesting properties. These structures have previously been described, both from simulation and experiment, by radial distribution functions for the various atomic pairs. Figures 3 and 4 give the pure DMSO radial distribution functions between heavy atoms and between heavy atoms and hydrogen atoms. The strong interactions between the DMSO oxygen atoms and methyl groups are demonstrated by both figures. The relatively long range of the liquid structure (~10 Å), resulting from the strong polar interactions and relatively large molecular size, can

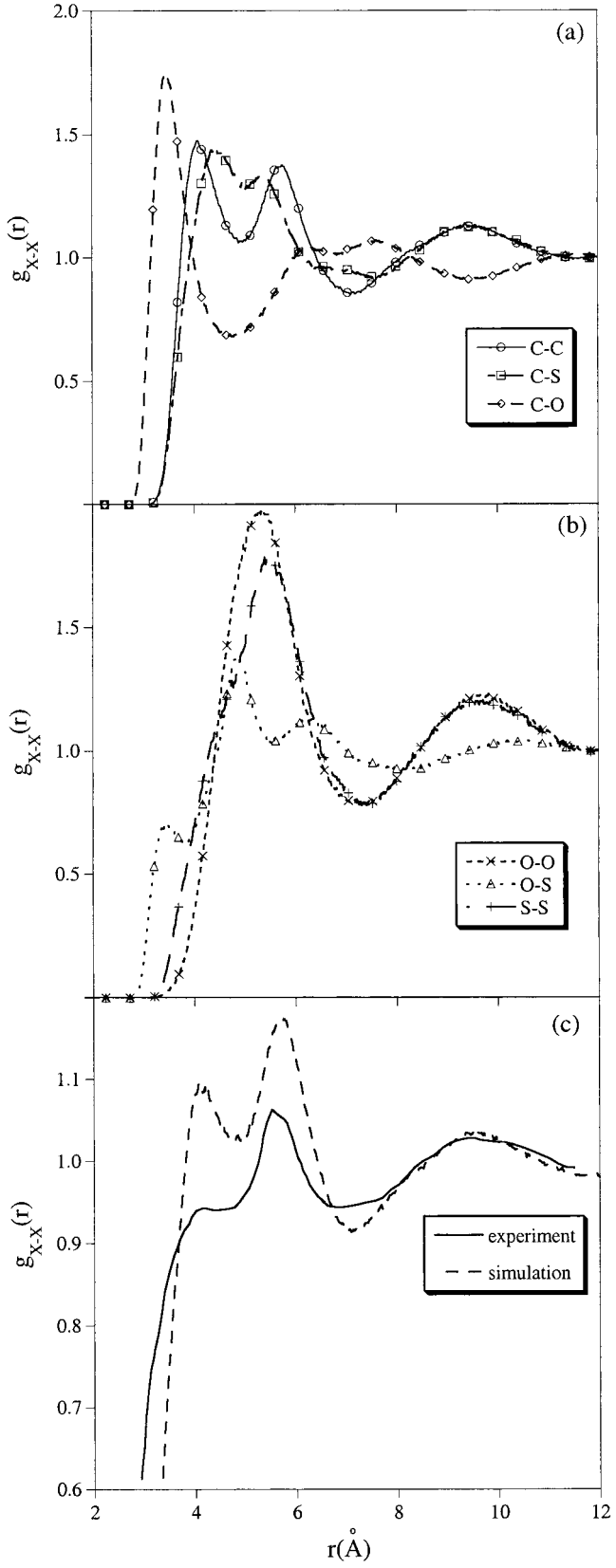

Figure 3. (a) Radial distribution functions for heavy atoms calculated from the neat DMSO simulation. (b) Radial distribution functions for heavy atoms calculated from the neat DMSO simulation. (c) Weighted radial distribution function for heavy atoms from experiment (solid) and simulation (dashed).

be seen from the simulation data in the upper panel. This result is in excellent agreement with experiment, as can be observed in the lower panel where the simulated distribution functions

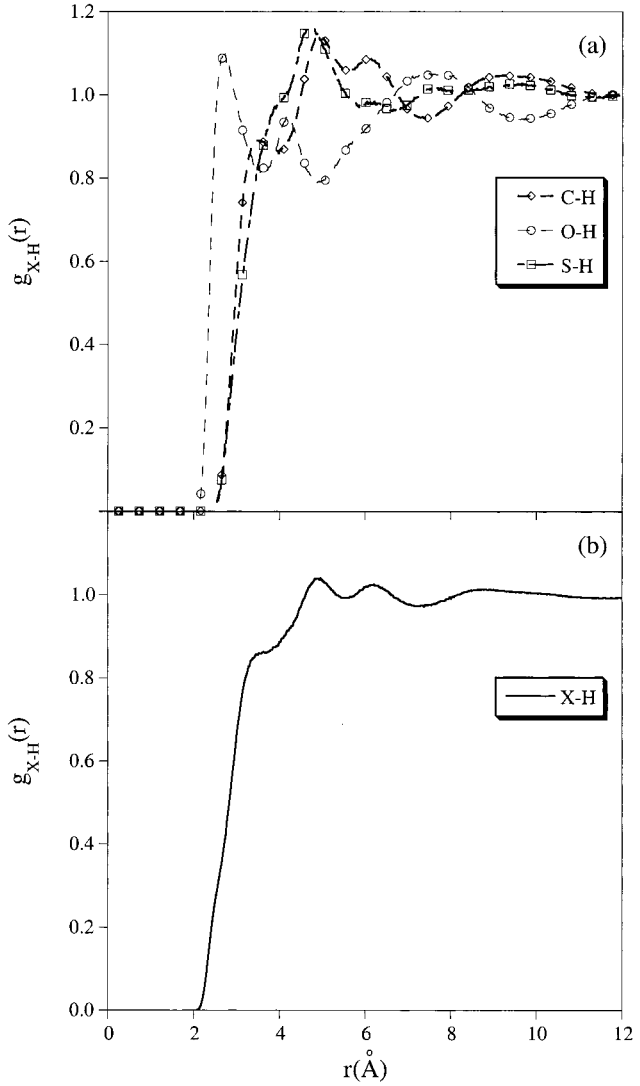

Figure 4. (a) Radial distribution functions for heavy atoms; hydrogen atoms calculated from the simulation of pure DMSO. (b) Weighted radial distribution function calculated from the data presented in Figure 4a, using the experimental weights of ref 15.

have been normalized using the experimental weighting factors given in ref 15. The location of all three local maxima is very well reproduced by the simulation. At short range the simulated liquid exhibits a higher degree of order than observed experimentally; however, this increased order is sufficiently small that the difference may be due to the limited resolution of the experiment. Similarly exaggerated order at short range has been observed in simulations using other models.[14] Comparison of Figure 4b of the present work (the heavy atom − hydrogen atom distribution function) with the experimentally determined $g(r)$ given in Figure 9 of ref 15 shows similarly good agreement to the fluid structure.

To study the effect of DMSO on water structure in the mixtures, an overlay of the water hydrogen−water hydrogen radial distribution functions for neat water and the two mixtures with DMSO are given in Figure 5. As the concentration of water decreases, its structure becomes enhanced. In the case of the 4:1 DMSO:water mixture, the effect is dramatic with a large increase at short range (corresponding to molecules that are hydrogen bonded to each other) and a depletion at intermediate distances (4−6 Å). Visualization of the simulation cell revealed the formation of short "chains" of hydrogen bonded waters. This finding could explain the extremely long rotational reorientation

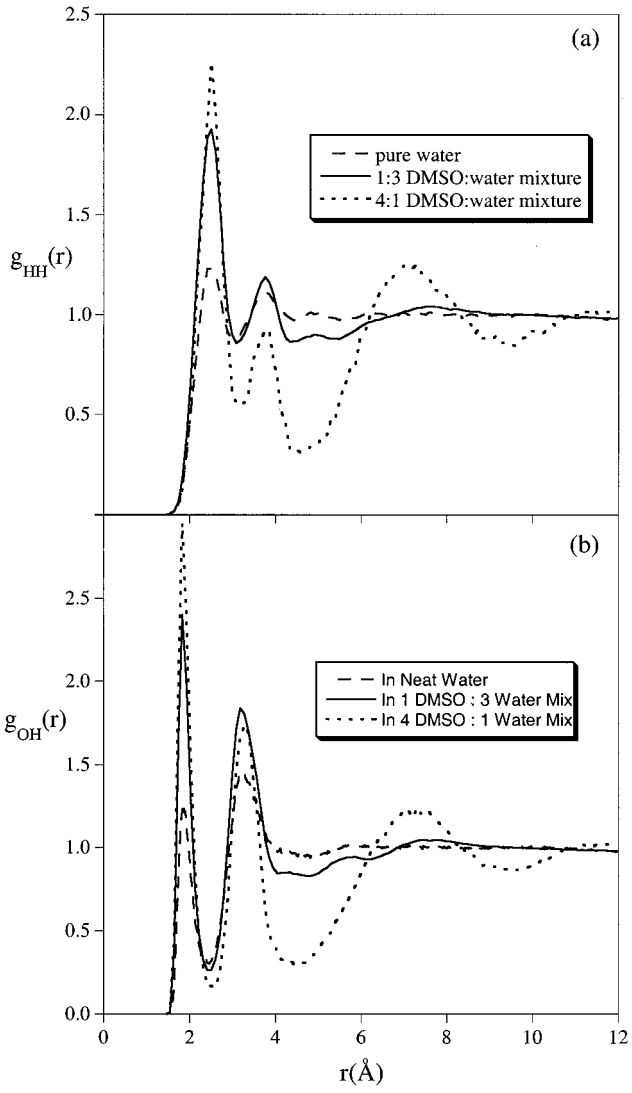

Figure 5. (a) $H_{H_2O}-H_{H_2O}$ radial distribution of neat TIP3P water and TIP3P water in DMSO solutions. (b) $O_{H_2O}-H_{H_2O}$ radial distribution of neat TIP3P water and TIP3P water in DMSO solutions.

relaxation time observed at this mixture concentration. The behavior of water also indicates it is an extremely competitive hydrogen bond acceptor at this concentration where the number of hydrogen bond donors is scarce. It should be emphasized that, due to the difference in molecular volumes, the water concentration is even lower than the 4:1 ratio suggests (although the mole percent water is 20%, the volume percent of water is less than 6%).

Conclusions

The present model is a significant change from previous models of DMSO, incorporating atomic flexibility and explicit representation of hydrogen atoms. These enhancements provide a solvent model that is consistent with modern parameter sets for the simulation of biomolecules and have been shown, for some systems, to be necessary for accurate descriptions of condensed phases. The present model has been tested against a range of experimental data for structural and dynamic properties and shown to be highly accurate. The existence of a high quality DMSO model, that is consistent with the CHARMM all-atom parameter sets for biomolecules, allows for the possibility of simulating many interesting systems. Additionally, the all-atom model presented here allows comparison with structural data available from neutron scattering experiments that probe the heavy atom − hydrogen atom structure within the fluid.

As noted by earlier developers of DMSO models, quantitative agreement with experiment for the entire range of experimentally measured properties is elusive. Previous workers had suggested that use of an all-atom model of DMSO might alleviate these discrepancies. The present work, which examined a large array of possible parameter combinations, is still the result of a compromise among agreement with various properties. It is possible that the goal of maintaining compatibility with the CHARMM parameter set prevented us from obtaining quantitative agreement with all properties. An alternative explanation is that a simple model based on fixed atomic charges is incapable of reproducing all the properties examined here and that the inclusion of polarizability is a necessary component of an accurate model of liquid-state DMSO.

Acknowledgment. We thank Professor Alexander MacKerell for helpful discussions and Dr. A. Vishnyakov for providing data for Figure 3. This work was supported by the National Science Foundation through award MCB-0091508.

References and Notes

(1) Becker, O. M.; MacKerell, A. D.; Roux, B.; Watanabe, M. *Computational Biochemistry and Biophysics*; Marcel-Dekker: New York, 2001.
(2) Feller, S. E. *Curr. Opin. Colloid Interface Sci.* **2000**, *5*, 217.
(3) Petrache, H. I.; Feller, S. E.; Nagle, J. F. *Biophys. J.* **1997**, *72*, 2237.
(4) Feller, S. E.;Huster, D.; Gawrisch K. *J. Am. Chem. Soc*. **1999**, *121*, 8963.
(5) Ahkong, Q. F.; Fischer D.; Tampion W.; Lucy, J. A. *Nature* **1975**, *253*, 194.
(6) Anchordoguy, T. J.; Carpenter, J. F.; Crowe, J. H.; Crowe, L. M. *Biochim. Biophys. Acta* **1992**, *1104*, 117.
(7) Lovelock, J. E.; Bishop, M. W. H. *Nature* **1959**, *183*, 1394.
(8) Milligan, J. R.; Ward, J. F. *Radiat. Res.* **1994**, *137*, 295.
(9) Baker, E. S.; Jonas, J. *J. Phys. Chem.* **1985**, *98*, 1730.
(10) Stafford, G. J.; Schaffer, P. C.; Leung, P. S.; Doebbler, G. F.; Brady, G. W.; Lyden, E. F. X. *J. Chem. Phys.* **1969**, *50*, 2140.
(11) Glasel, J. A. *J. Am. Chem. Soc.* **1970**, *92*, 372.
(12) Kowalewski, J.; Kovacs, H. Z. *Phys. Chem. Board* **1986**, *149*, 49.
(13) Rasmussen, D.; MacKenzie, A. P. *Nature* **1968**, *220*, 1315.
(14) Vishnyakov, A.; Lyubartsev, A. P.; Laaksonen, A. *J. Phys. Chem. A* **2001**, *105*, 1702.
(15) Luzar, A.; Soper, A. K.; Chandler, D. *J. Chem. Phys.* **1993**, *99*, 6836.
(16) Liu, H.; Müller-Plathe, F.; van Gunsteren, W. F. *J. Am. Chem. Soc.* **1995**, *117*, 4363.
(17) Vaisman, I. I.; Berkowitz, M. L. *J. Am. Chem. Soc.* **1992**, *114*, 1889.
(18) Luzar, A.; Chandler, D. *J. Chem. Phys.* **1993**, *98*, 8160.
(19) Paci, E.; Marchi, M. *Mol. Simul.* **1994**, *14*, 1−10.
(20) Smondyrev, A. M.; Berkowitz, M. L. *Biophys. J.* **1999**, *76*, 2372.
(21) Rao, B. G.; Singh, U. C. *J. Am. Chem. Soc.* **1990**, *112*, 3803.
(22) Brooks, B. R.; Bruccoleri, R. E.; Olafson, B. D.; States, D. J.; Swaminathan, S.; Karplus, M. *J. Comput. Chem.* **1983**, *4*, 187.
(23) MacKerell, A. D., Jr.; Brooks, B.; Brooks, C. L., III; Nilsson, L.; Roux, B.; Won, Y.; Karplus, M. CHARMM: The Energy Function and Its Parametrization with an Overview of the Program. In *Encyclopedia of Computational Chemistry*; Schleyer, P. v. R., Clark, N. L. A., T., Gasteiger, J., Kollman, P. A., Schaefer, H. F., III, Schreiner, P. R. S, Eds.; John Wiley & Sons: Chichester, 1998; Vol. 1, pp 271−277.
(24) Schlenkrich, M.; Brickmann, J.; MacKerell, A. D., Jr.; Karplus, M. In *Biological Membranes; A Molecular Perspective from Computation and Experiment*; Merz, K. M.; Roux, B., Eds.; Birkhaüser: Boston, 1996; pp 31−81.
(25) Frisch, M. J.; Trucks, G. W.; Schlegel, H. B.; Scuseria, G. E.; Robb, M. A.; Cheeseman, J. R.; Zakrzewski, V. G.; Montgomery, J. A., Jr.; Stratmann, R. E.; Burant, J. C.; Dapprich, S.; Millam, J. M.; Daniels, A. D.; Kudin, K. N.; Strain, M. C.; Farkas, O.; Tomasi, J.; Barone, V.; Cossi, M.; Cammi, R.; Mennucci, B.; Pomelli, C.; Adamo, C.; Clifford, S.; Ochterski, J.; Petersson, G. A.; Ayala, P. Y.; Cui, Q.; Morokuma, K.; Malick, D. K.; Rabuck, A. D.; Raghavachari, K.; Foresman, J. B.; Cioslowski, J.;

Ortiz, J. V.; Stefanov, B. B.; Liu, G.; Liashenko, A.; Piskorz, P.; Komaromi, I.; Gomperts, R.; Martin, R. L.; Fox, D. J.; Keith, T.; Al-Laham, M. A.; Peng, C. Y.; Nanayakkara, A.; Gonzalez, C.; Challacombe, M.; Gill, P. M. W.; Johnson, B. G.; Chen, W.; Wong, M. W.; Andres, J. L.; Head-Gordon, M.; Replogle, E. S.; Pople, J. A. *Gaussian 98*, Gaussian, Inc.: Pittsburgh, PA, 1998.

(26) PCSpartanPro, Wavefunction, Inc., 18401 Von Karman, Suite 370, Irvine, CA, 92612.

(27) Foresman, J. B.; Frisch, Æ. *Exploring Chemistry with Electronic Structure Methods*, 2nd ed.; Gaussian, Inc.: Pittsburgh, PA, 1993; p 64.

(28) Chirlian, L. E.; Francl, M. M. *J. Comput. Chem*. **1987**, *8*, 894.

(29) MacKerell, A. D., Jr.; Karplus, M. *J. Phys. Chem.* **1991**, *95*, 10559−10560.

(30) Feller, S. E.; Pastor, R. W.; Rojnuckarin, A.; Bogusz, S.; Brooks, B. R.; *J. Phys. Chem.* **1996**, *100*, 17011.

(31) Essman, U.; Perera, L.; Berkowitz, M. L.; Darden, T.; Lee, H.; Pedersen, L. G. *J. Chem. Phys*. **1995**, *103*, 8577−8593.

(32) Ryckaert, J. P.; Ciccotti, G.; Berendsen, H. J. C. *J. Comput. Phys.* **1977**, *23*, 327.

(33) Feller, S. E.; Zhang, Y.; Pastor, R. W.; Brooks, B. R. *J. Chem. Phys.* **1995**, *103*, 4613.

(34) Hoover, W. G. *Phys. Rev. A* **1985**, *31*, 1695−1697.

(35) Pastor, Richard W. In *Encyclopedia of Computational Chemistry*; John Wiley and Sons: New York, 1998; pp 3003−3011.

(36) Helfand, E. *Phys. Rev.* **1960**, *119*, 1.

(37) Press: W. H.; Teukolsky, S. A.; Vettering, W. T.; Flannery, B. P. *Numerical Recipies*; Cambridge University Press: New York, 1992.

(38) Allen, M. P.; Tildesley, D. J. *Computer Simulation of Liquids*; Clarendon: Oxford, U.K., 1987.

(39) MacKerell, A. D., Jr.; Bashford, D.; Bellott, M.; Dunbrack, R. L., Jr.; Evanseck, J.; Field, M. J.; Fischer, S.; Gao, J.; Guo, H.; Ha, S.; Joseph, D.; Kuchnir, L.; Kuczera, K.; Lau, F. T. K.; Mattos, C.; Michnick, S.; Ngo, T.; Nguyen, D. T.; Prodhom, B.; Reiher, W. E., III.; Roux, B.; Schlenkrich, M.; Smith, J.; Stote, R.; Straub, J.; Watanabe, M.; Wiorkiewicz-Kuczera, J.; Yin, D.; Karplus, M. *J. Phys. Chem. B* **1998**, *102*, 3586−3616.

(40) Zheng, Y. J.; Ornstein, R. L. *J. Am. Chem. Soc.* **1996**, *118*, 4175.

(41) Thomas, R.; Schoemaker, C. B.; Erics, K. *Acta Crystallogr*. **1966**, *21*, 12.